J. Eng. Sci., Univ. Riyadh, Vol. 7 (1), pp. 53 - 63 (1981)

Analysis of Variable Frequency Inverter– Induction Motor System

M.A. Shimy Mansour* (Late), M.A. Alhaider and I.Fatoh*****

* *Late Professor of Electrical Engineering, College of Engineering, University of Riyadh, Riyadh, Saudi Arabia;*

** *Assistant Professor of Electrical Engineering, College of Engineering, University of Riyadh, Riyadh, Saudi Arabia; and*

*** *Electrical Engineering Department, Faculty of Engineering, Cairo University, Egypt.*

For an inverter-fed induction motor the constraints for the different modes of operation change many times during a cycle. This is a source of difficulty in analyzing the transient and steady-state electromechanical performance of the machine. All the available methods such as the multiple reference frames, equivalent circuit approach and matrix approach idea assume the shape of the phase voltage beforehand. Investigation has shown that the assumption of a known voltage, as in case of a resistive load, is not sufficiently accurate for current waveform and instantaneous torque determination.

A new digital computer model of a variable frequency, inverter-fed induction motor system, based on tensor analysis approach is presented in this paper. This model can be used to predict the performance of the aforementioned system under controlled-slip, variable speed operating conditions. It can also be used to optimize system performance.

The paper provides experimental results in verification of the predicted digital computer performance figures for both symmetrical and asymmetrical operation of the system.

List of Symbols

a, b, c Subscripts referring to rotor phases

A, B, C, Subscripts referring to stator phases

$[A]^{-1}$ Inverse of matrix [A]

C_f Filter capacitance

$[C]^T$ Transpose of connection matrix [C]

$[C_V]_n$ Defined matrix

E Inverter dc input voltage

f Frequency, function

$[G_{(W^r)}]$ Speed dependent impedance matrix

i Instantaneous current

[i] General current vector

$[i_{(o)}]$ Initial current vector

$[i_{(n)}]$ Current vector at time interval (n Δ t)

i_a, i_b, i_c Rotor currents referred to stator

i_a^r, i_b^r, i_c^r Actual rotor currents

i_α, i_β, i_γ Stator currents

J & k, K Angular moment of inertia and Integers

[L] Speed independent inductance matrix

L_f Filter inductance

L_s Source inductance

L^s Self inductance of one stator phase

L_p^r Effective rotor self inductance of one phase referred to rotor

m Subinterval number

n Interval number

P Subscript of referring to primitive parameters

p Number of pole pairs

$\mathfrak{p}$ $\frac{d}{dt}$

r Superscript referring to rotor parameters

R Resistance

R_f Filter resistance

R_s Source input resistance

s Superscript referring to stator parameters

t & t_c Time and Conduction time of thyristor

Δt Time interval

T Electromagnetic torque

T_L & [U] Load torque and unit matrix

v Instantaneous phase voltage

[V] General voltage vector

$\bar{V}_s$ Forcing function

w Electrical angular frequency

x_1, x_2 State variables

α Thyristor firing angle

ϵ Inverter terminal voltage

$[\psi]$ Instantaneous inductance matrix

λ ψi

θ Rotor angular displacement

$\dot{\theta}$ Rotor angular speed

1. Introduction

The inverter – induction motor systems are becoming of increased practical use. Therefore, a need arised for an improved digital computer model for calculating the dynamic and the steady-state behaviour of such systems.

The constraints imposed on induction motor modes of operation change many times during a cycle and considerable difficulty is encountered in analyzing the electromechanical transient or steady state conditions.

All the available methods such as multiple reference frames, equivalent circuit approach and others [1–8] assume the shape of the phase voltage. In reality, then such methods use the ideal inverter voltage in case of resistive load as an ideal voltage for the inductive load and induction motor load.

The investigation shows that the assumption of a known voltage, as in case of a resistive load, is not sufficiently accurate for current waveform and instantaneous torque determination [9].

A new digital model based on tensor analysis approach, is proposed to calculate the inverter-induction motor system behaviour without the need to assume the shape of the inverter output phase-voltage. Hence the model is generalized to handle other cases such as converter-inverter induction motor system and cycloconverter – induction motor system considering filter and source impedances.

Torque pulsations are investigated for different cases and compared in cases of symmetrical and asymmetrical operation.

2. Basic Equation

The following voltage equation is applicable to each winding of stator and rotor of three phase induction motor:

$$V = \mathrm{p}\,\lambda + Ri \qquad (1)$$

The basic equation is obtained by using the concept of power invariance [10]. Its basic tenet is to transform the time dependent equation (1) to time independent equation in a way similar to the direct and quadrature axes transformations [3, 6]. However, the transformation is done without change in stator variables so that (a) these quantities may easily be obtained and (b) the focred inverter terminal constraints could be applied to the equation. The variable stator-to-rotor mutual inductances can be made independent of rotor phase position w.r.t. stator phases by transforming the rotor quantities to a stationary reference frame as summarized in appendix (A).

Equations of five variables are obtained without hindering the physical meaning behind these equations. These variables can be arranged and put in the following abstract notations:

$$[V]_p = [G_{(W^r)}]_p\,[i]_p + [L]_p\,\mathrm{p}\,[i]_p \qquad (2)$$

where;

$$[V]_p = \begin{bmatrix} V_A+V_B+V_C \\ V_A-V_C \\ V_C-V_B \\ 0 \\ 0 \end{bmatrix}, \quad [i]_p = \begin{bmatrix} i_o \\ i_\alpha \\ i_\beta \\ i_a \\ i_b \end{bmatrix} \qquad (2a)$$

$$[G_{(W^r)}] = \begin{bmatrix} 3R^S & 0 & 0 & 0 & 0 \\ 0 & 2R^S & R^S & 0 & 0 \\ 0 & R^S & 2R^S & -\sqrt{3}Mw^r & 0 \\ 0 & 0 & \sqrt{3}Mw^r & 2R^r & R^r+\frac{3\sqrt{3}}{2}L_p^r w^r \\ 0 & 0 & 0 & R^r-\frac{3\sqrt{3}}{2}L_p^r w^r & 2R^r \end{bmatrix} \qquad (2b)$$

$$\text{and } [L]_p = \begin{bmatrix} 3L^s_o & 0 & 0 & 0 & 0 \\ 0 & 3L^s_p & \frac{3}{2}L^s_p & 2M & M \\ 0 & 3/2\,L^s_p & 3L^s_p & M & 2M \\ 0 & 2M & M & 3L^r_p & \frac{3}{2}L^r_p \\ 0 & M & 2M & \frac{3}{2}L^r_p & 3L^r_p \end{bmatrix} \quad (2c)$$

This equation is arranged in a form, so that normal constraints upon the voltage of the machine, imposed by the known inverter switching connections, can be directly applied. In addition, the solution for the dependent current variables can be easily interpreted in terms of the phase currents. Therefore, equations (2) are taken as primitive equations for inverter–induction motor system. With the basis of tensor analysis [11] the phase voltage is not assumed as in the previous methods [1–8].

3. Method of Analysis

With many inverter modes, the voltage applied to the motor phases is obtained by a series of thyristor switchings for the phases across a D C source periodically. The most common example is the six interval inverter system.

The motor equation for each interval can be obtained by using the connection matrix between the primitive system and the interval system as in the following:

Interval «1»

Thyristors, 1, 4 and 6 in Fig. (1) are ON as shown in Fig. (2b). The rotor has the same connection for all intervals similar to the primitive connection. Therefore, the connection matrix $[C]_1$ between the primitive variables in equation (2) and the new variables shown in Fig. (2b), can be written by comparing Fig. (2a) with Fig. (2b) as:

$$[i]_p = [C]_1\,[i]_1 \quad (3)$$

or

$$\begin{bmatrix} i_\alpha \\ i_a \\ i_\beta \\ i_b \end{bmatrix} = \begin{bmatrix} 1 & 0 & 0 & 0 \\ 0 & -1 & 0 & 0 \\ 0 & 0 & 1 & 0 \\ 0 & 0 & 0 & 1 \end{bmatrix} \begin{bmatrix} i_1 \\ i_2 \\ i_a \\ i_b \end{bmatrix} \quad (4)$$

Applying the tensor basis (4) to equations (2) and (3) yields:

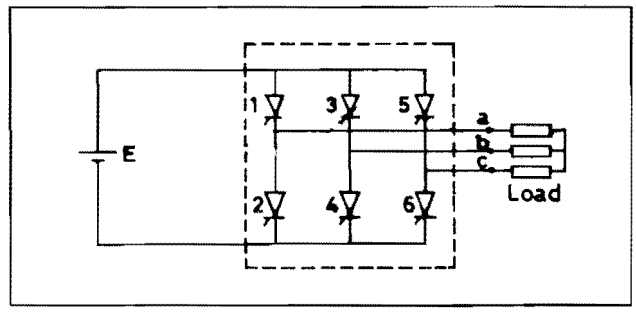

Fig. (1). Stepped wave inverter

$$[V]_1 = [G_{(W^r)}]_1\,[i]_1 + [L]_1\,P\,[i]_1 \quad (5)$$

where

$$[V]_1 = [C]^T_1\,[V]_p = \begin{bmatrix} V_A - V_C \\ V_B - V_C \\ \\ 0 \\ 0 \end{bmatrix} = \begin{bmatrix} E \\ 0 \\ \\ 0 \\ 0 \end{bmatrix} \quad (5a)$$

$$[G_{(W^r)}]_1 = [C]^T_1\,[G_{(W^r)}]_p\,[C]_1 \quad (5b)$$

and

$$[L]_1 = [C]^T_1\,[L]_p\,[C]_1 \quad (5c)$$

Interval «2»

Thyristors 1, 3 and 6 in Fig. (1) are ON as shown in Fig. (2c). The choice of the new variables is similar to interval «1», hence, the connection matrix $[C]_2$ is similar to $[C]_1$ and by the same way we get:

$$[V]_2 = [G_{(W^r)}]_1\,[i]_2 + [L]_1\,P[i]_2 \quad (6)$$

where

$$[V]_2 = \begin{bmatrix} V_A - V_C \\ V_B - V_C \\ \\ 0 \\ 0 \end{bmatrix} = \begin{bmatrix} E \\ E \\ \\ 0 \\ 0 \end{bmatrix} \quad (6a)$$

Interval «3»

Thyristors 3, 2 and 6 in Fig. (1) are ON as shown in Fig. (2d). As before, the following equation is obtained:

$$[V]_3 = [G_{(W^r)}]_1\,[i]_3 + [L]_1\,P\,[i]_3 \quad (7)$$

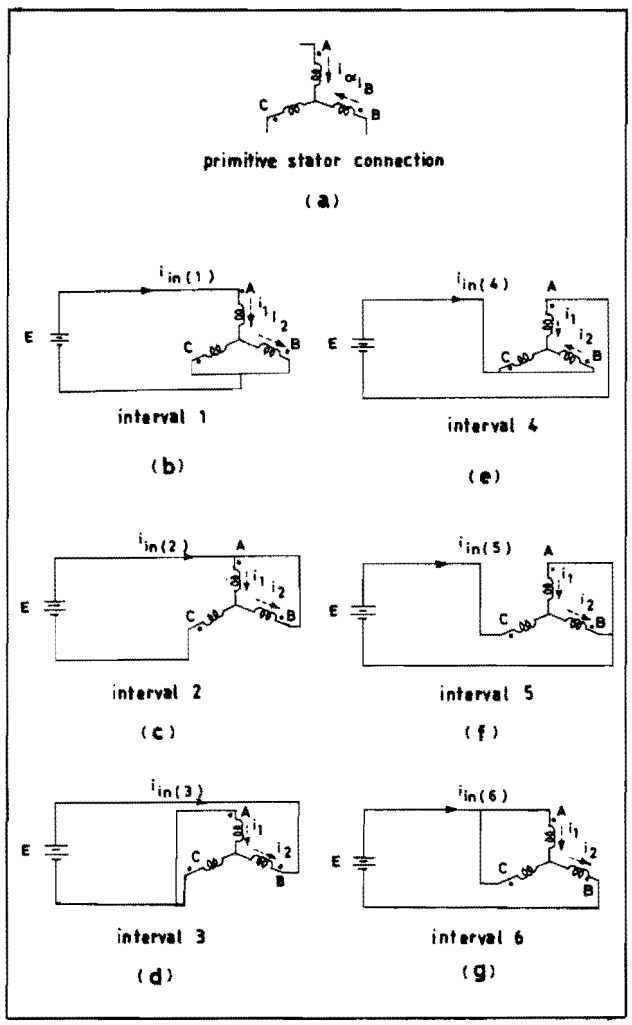

Fig. (2). Six interval connections

where

$$[V]_3 = \begin{bmatrix} V_A - V_C \\ V_B - V_C \\ \\ 0 \\ 0 \end{bmatrix} = \begin{bmatrix} 0 \\ E \\ \\ 0 \\ 0 \end{bmatrix} \qquad (7a)$$

Interval «4»

Thyristor 3, 5 and 2 in Fig. (1) are ON as shown in Fig. (2e). As before, the equation will be:

$$[V]_4 = [G_{(W^r)}]_1 [i]_4 + [L]_1 \, ₱ \, [i]_4 \qquad (8)$$

where

$$[V]_4 = \begin{bmatrix} V_A - V_C \\ V_B - V_C \\ \\ 0 \\ 0 \end{bmatrix} = \begin{bmatrix} -E \\ 0 \\ \\ 0 \\ 0 \end{bmatrix} \qquad (8a)$$

Interval «5»

Thyristors 2, 5 and 4 in Fig.(1) are ON as shown in Fig. (2f). The equation will be:

$$[V]_5 = [G_{(W^r)}]_1 [i]_5 + [L]_1 \, ₱ \, [i]_5 \qquad (9)$$

where

$$[V]_5 = \begin{bmatrix} V_A - V_C \\ V_B - V_C \\ \\ 0 \\ 0 \end{bmatrix} = \begin{bmatrix} -E \\ -E \\ \\ 0 \\ 0 \end{bmatrix} \qquad (9a)$$

Interval «6»

Thyristors 1, 4 and 5 in Fig. (1) are ON as shown in Fig. (2g). The equation will be:

$$[V]_6 = [G_{(W^r)}]_1 [i]_6 + [L]_1 \, ₱ \, [i]_6 \qquad (10)$$

where

$$[V]_6 = \begin{bmatrix} V_A - V_C \\ V_B - V_C \\ \\ 0 \\ 0 \end{bmatrix} = \begin{bmatrix} 0 \\ -E \\ \\ 0 \\ 0 \end{bmatrix} \qquad (10a)$$

4. Mathematical Model

A general model is proposed to solve the inverter–induction motor system permitting a convenient and simple method of analyzing steady state modes as well as transient processes, considering speed pulsations in case of symmetrical and asymmetrical triggering. Equations (5) through (10) can be rearranged as follows:

$$₱ \, [i]_n = [L]_1^{-1} [G_{(W^r)}] [i]_n + [L]_n^{-1} [V]_n \qquad (11)$$

The solution to equation (11) for any time ($n \Delta t$) expressed in terms of the system initial conditions at ($n-1$) Δt is given by [12]:

$$[i_{(n)}]_n = e^{[A(n)]\Delta t} [i_{(n-1)}]_{n-1} + \left[[U] - e^{[A(n)]\Delta t}\right] [G_{(n)}]^{-1} [V]_n \qquad (12)$$

where

$$[A_{(n)}] = - [L]_1^{-1} [G_{(n)}]_1 \qquad (12a)$$

and

$$[G_{(n)}] = [G_{(W^r{}_n)}]_1 \qquad (12\,b)$$

To apply equations (12), it is necessary to find the initial current vector $[i_{(n-1)}]$ assuming the speed is constant for each interval.

Equation (12) can be used with more accuracy when each interval is divided to subintervals (K) as:

$$[i_{(nK+m)}]_{n+1} = e^{[A_{(nk+m)}]\Delta t}\ [i_{(nK+m-1)}] + \left[[U] - e^{[A_{(nk+m)}]\Delta t}\right]\ [G_{(nK+m)}]^{-1}[V]_{n+1} \quad (13)$$

where

$$m = 0, 1, 2, \ldots\ldots K \text{ subintervals} \quad (13\ a)$$

and

$$n = 0, 1, 2, \ldots\ldots N \text{ intervals} \quad (13\ b)$$

Once the induction motor currents are calculated, the inverter input current can be evaluated simply by using the interval relation matrices 1 to 6 derived from Fig. (2) as follows:

Interval «1»

$$i_{in(1)} = [1 \quad 0] \begin{bmatrix} i_1 \\ i_2 \end{bmatrix}_1 \quad (14a)$$

Interval «2»

$$i_{in(2)} = [1 \quad -1] \begin{bmatrix} i_1 \\ i_2 \end{bmatrix}_2 \quad (14b)$$

Interval «3»

$$i_{in(3)} = [0 \quad -1] \begin{bmatrix} i_1 \\ i_2 \end{bmatrix}_3 \quad (14c)$$

Interval «4»

$$i_{in(4)} = [-1 \quad 0] \begin{bmatrix} i_1 \\ i_2 \end{bmatrix}_4 \quad (14d)$$

Interval «5»

$$i_{in(5)} = [-1 \quad 1] \begin{bmatrix} i_1 \\ i_2 \end{bmatrix}_5 \quad (14\ e)$$

Interval «6»

$$i_{in(6)} = [0 \quad 1] \begin{bmatrix} i_1 \\ i_2 \end{bmatrix}_6 \quad (14f)$$

where $i_{in(1)}$ to $i_{in(6)}$ represent the currents during intervals 1 to 6 respectively.

5. Application of The New Digital Model

A digital computer is used to solve equations (13) and (14) with emphasis on two major applications, namely, steady-state and transient-state for symmetrical and asymmetrical triggering.

5.1 Symmetrically Triggered Thyristors

For symmetrically triggered thyristors equation (13) is used with equal time intervals. In addition to equation (13), the dynamic behaviour of the system can be studied by the equation governing the change of rotor speed as:

$$P\ \dot{\theta}_n = \left[[i_{(n)}]^T\ [G_{(n)}] - [R]\ [i_{(n)}]\right] \frac{P}{Jw^r} - \frac{T_L}{J} \quad (15)$$

The differential equation (15) can be arranged in a form suitable for digital computation by using any numerical method such as Runge-Kutta method or Predictor-corrector method, etc. If the Predictor-corrector method is used, equation (15) can be rearranged in the following form:

$$\dot{\theta}^0\ (nK+m+1) = \dot{\theta}\ (nK+m) + \Delta t\ P\ \dot{\theta}\ (nK+m) \quad (16)$$

$$\dot{\theta}^1(nK+m+1) = \frac{\dot{\theta}\ (nK+m) + \dot{\theta}^0(nK+m+1)}{2} + \frac{\Delta t}{2} P\theta^0(nK+m) \quad (17)$$

$$\dot{\theta}^k(nK+m+1) = \frac{\dot{\theta}\ (nK+m) + \dot{\theta}^{k-1}\ (nK+m+1)}{2} + \frac{\Delta t}{2}\ P\ \dot{\theta}^{k-1}\ (nK+m) \quad (18)$$

The iteration is terminated when two successive iterations converge to the desired accuracy.

The system of equations (13), (16), (17) and (18) can be solved by introducing the initial values for the currents and rotor speed. Hence, these equations are suitable to solve any sudden change. Also it can be used to get the steady-state solution whether the speed is constant or not.

5.2 Asymmetrically Triggered Thyristors

For practical reasons the inverter-induction motor system may have asymmetrical triggered wave as shown in Fig. (3). Equations (13), (16), (17) and (18) must be modified so that the lengthened interval and the shortened interval have the correct number of sub-intervals. This may be done as follows, take for example, an interval (n) as lengthened one and (n+1) as a shortened one as shown in Fig. (3). The program must be designed so that interval (n) has a number of

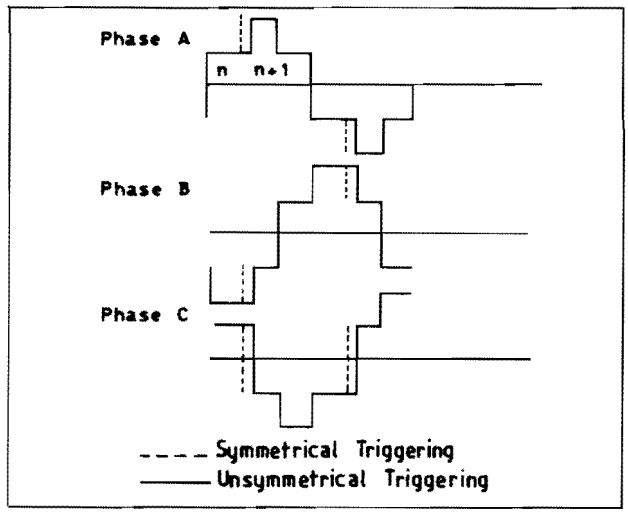

Fig. (3). Symmetrical triggering and asymmetrical triggering

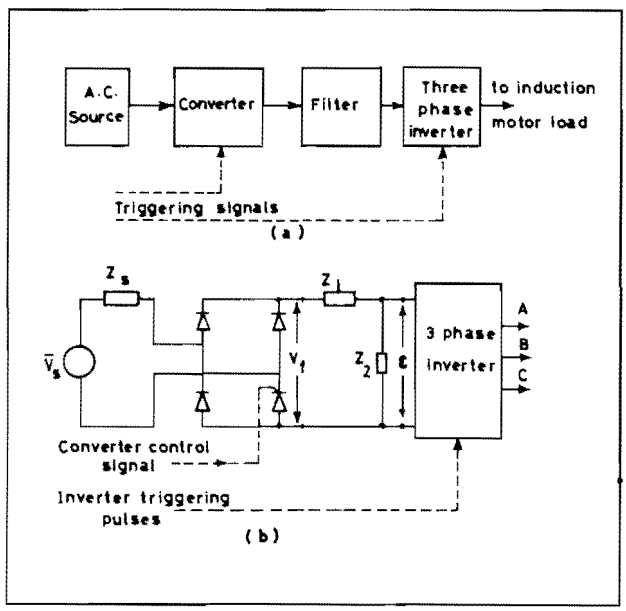

Fig. (4). Converter inverter induction motor system

sub-intervals higher than K and interval (n+1) has a number of sub-intervals less than K. By doing this the solution is obtained using equations (13), (16), (17) and (18) respectively.

5.3 Application to the Analysis of a Converter-Inverter Induction Motor Drive

The new digital model is employed to establish a method for calculating the inverter-induction motor variables when supplied by any voltage shape. In converter-inverter system, the input inverter voltage depends on the inverter-induction motor variables because of filter and source impedances as shown in Fig. (4). The equivalent circuit and equivalent source voltage are shown in Fig. (5). The equation describing the system shown in Fig. (5), is derived as follows:

$$\bar{V}_{S(n)} = (R+L\mathrm{P})\,(i_{in(n)} + C_f \mathrm{P}\varepsilon) \qquad (19)$$

where

$$R = R_S + R_f \text{ and } L = L_S + L_f \qquad (19\ a)$$

The inverter input currents can be expressed in terms of the motor phase currents by using equation (14) after being put in the following form:

$$i_{in(n)} = [C]_n\,[i]_n \qquad (20)$$

where

$$\begin{bmatrix}[C]_1\\ [C]_2\\ [C]_3\\ [C]_4\\ [C]_5\\ [C]_6\end{bmatrix} = \begin{bmatrix}1 & 0 & 0 & 0\\ 1 & -1 & 0 & 0\\ 0 & -1 & 0 & 0\\ -1 & 0 & 0 & 0\\ -1 & 1 & 0 & 0\\ 0 & 1 & 0 & 0\end{bmatrix} \qquad (20\ a)$$

Combining equations (19) and (20) and using equation (11) for the vector $\mathrm{P}(i)$ yield.

$$\bar{V}_{s(n)} = \left[R[C]_n + L[C]_n\,[L]_1^{-1}\,[G_{(W^r)}]\right][i]_n + L\,[C]_n\,[L]_n^{-1}\,[C_V]_n\,\varepsilon + R\,C_f \mathrm{P}\varepsilon + L\,C_f \mathrm{P}^2\varepsilon \qquad (21)$$

where, $[C_V]_n\ \varepsilon = [V]_n$ (21 a)

The second order differential equation (21) can be rewritten as a set of two first-order differential equations by using the state-space approach (12). A set of state variables sufficient to describe this system is the inverter terminal voltage (ε) and its rate of change ($\mathrm{P}\varepsilon$). Therefore, we will define a set of state variables as (x_1, x_2) where:

$$x_1(t) = \varepsilon(t) \quad \text{and} \quad x_2(t) = \mathrm{P}\varepsilon(t) \qquad (22)$$

Equation (21) can be written in terms of the state variables as follows:

$$\mathrm{P}\,x_1 = x_2 \qquad (23)$$

$$\mathrm{P}\,x_2 = \left[-\frac{R}{LC_f}[C]_n + \frac{1}{C_f}[C]_n\,[L]_1^{-1}\,[G_{(W^r)}]\right][i]_n - \frac{1}{C_f}[C]_N\,[L]_n^{-1}\,[C_v]_n\,x_1 - \frac{R}{L}\,x_2 + \frac{\bar{V}_{S(n)}}{LC_F} \qquad (24)$$

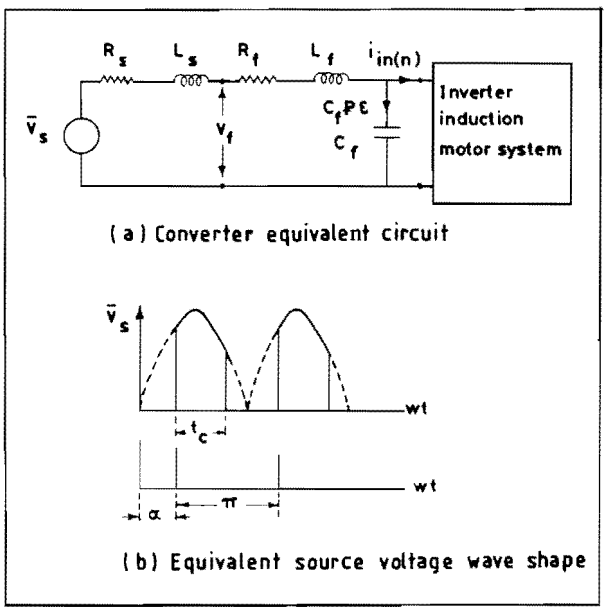

Fig. (5). (a) Converter equivalent circuit
(b) Equivalent source voltage wave shape

Thus this set of simultaneous differential equations may be written in matrix form as follows:

$$p\begin{bmatrix} x_1 \\ x_2 \end{bmatrix} = \begin{bmatrix} 0 & 1 & 0 \\ -\frac{1}{C_f}[C]_n[L]_n^{-1}[C_V]_n & -\frac{R}{L} & -\frac{R}{LC_f}[C]_n + \frac{1}{C_f}[C]_n[L]_1^{-1}[G_{(W.r_1)}] \end{bmatrix} \begin{bmatrix} x_1 \\ x_2 \\ [i]_n \end{bmatrix} + \begin{bmatrix} 0 \\ 1 \\ \overline{LC_f} \end{bmatrix} \bar{V}_s(n) \quad (25)$$

Equations (25), (11) and (14) form a perfect and complete model for converter–inverter induction motor system which can be solved as follows:

The forcing functions ($\bar{V}_S$) is known according to the known A.C. supply voltage and the converter firing angle (α). Because of converter effect, this forcing function ($\bar{V}_S$) is a sinusoidal function that is repeated every half cycle with respect to the frequency of the A.C. supply. The acting time (t_c) of the forcing function ($\bar{V}_S$) begins with the firing time of the converter and is continous as long as the current through the conducting thyristor is positive. Once the thyristor current goes to zero, the forcing function becomes zero and will continue to be zero until the start of the second firing time and so on. The thyristor conduction time (t_c) is affected by the forcing function which is the load torque.

In short, the system of equations (11), (14) and (25) are summarized as a set of simultaneous differential equations as follows:

$$P\begin{bmatrix} x_1 \\ x_2 \\ i \\ \theta \end{bmatrix} = \begin{bmatrix} f(x_1, x_2, [i], \theta, t) \end{bmatrix} + \begin{bmatrix} f(\bar{V}_S, T_L) \end{bmatrix} \quad (26)$$

It is evident that the computer programme utilizing the mentioned approach is still not complicated. This justifies its implementation for the study of converter–inverter systems.

The digital computer model presented can be used to predict the interaction between the load and the source of a converter–inverter system taking into account the effects of filters and series impedances.

6. Comparison of results

The experimental torque oscillograms for the case of imperfect symmetrical triggering as shown in Fig. (6), has the fundamental torque pulsations superimposed on the sixth harmonic. The experimantal oscillograms for the case of perfect triggering as depicted in Fig. (8) show the sixth harmonic torque pulsations only. This is also indicated by the digital computer results as shown in Fig. (7).

The reason behind the unexpected torque pulsations as depicted in the experimental oscillograms of Fig. (6) can be obtained from the digital model results of Figs. (9), (10) and (11) for different degrees of asymmetry. These figures show that the motor torque pulsations are very sensitive to the degree of asymmetry in triggering. In Fig. (11) for example, an asymmetry of 2.5° in one interval resulted in the modulation of the six pulse torque wave by a double amplitude fundamental wave. In Fig. (10) however, an asymmetry of 2.5° in each interval led to a distortion of the six pulse wave.

7. Conclusion

An inverter requires direct knowledge of the state of its phase quantities. The proposed transformation of the machine equations retains the stator phase variables while eliminating the time and position dependence of the machine inductance parameters. Therefore, this transformation expedites the

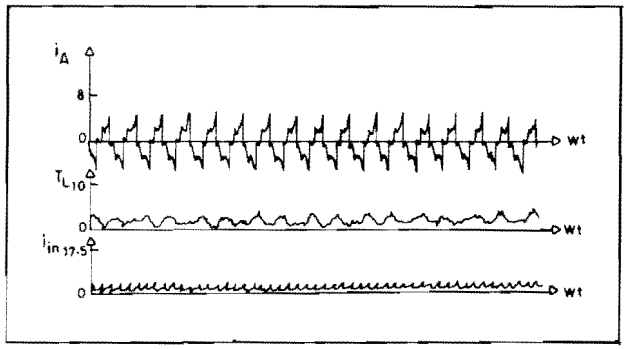

Fig. (6) Experimental oscillograms for symmetrical triggering f = 50 Hz θ = 1370 rpm

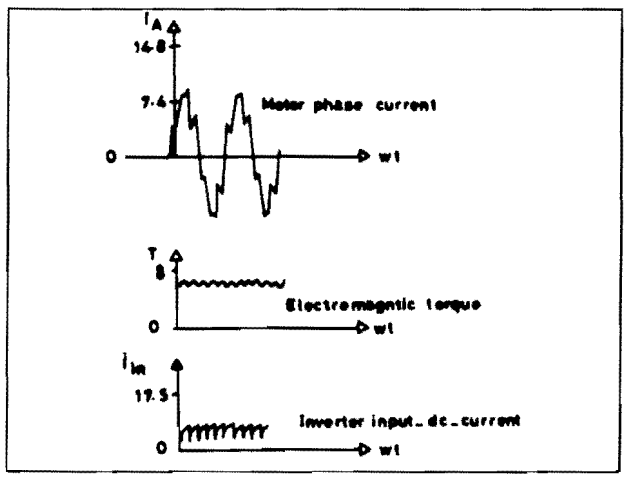

Fig. (7). New digital model results for: symmetrical triggering θ = 1370 rpm f = 50 Hz E = 180 V

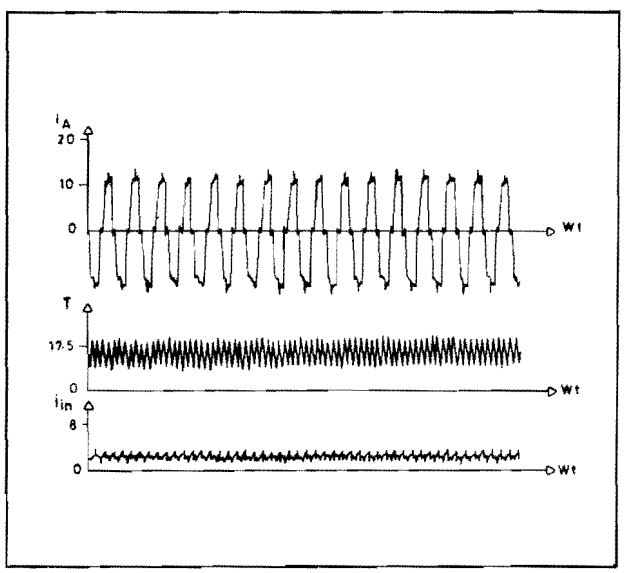

Fig. (8). Experimental oscillograms for symmetrical triggering (perfect) F = 40 Hz θ = 950 rpm

matching of the output terminal conditions of the inverter to the input terminal conditions of the induction motor and this in turn expedites the matching of the output terminal conditions of the converter or the DC source to the input terminal conditions of the inverter for any operating type, while retaining computational simplicity. Thus it is evident that the model is useful for evaluating the transient and dynamic performance of the induction motor in case of symmetrical or asymmetrical inverter operation. The model lends itself to easy manipulation, taking into account the source constraints and operating conditions of the converter and inverter. Detailed equations derived in a form which is directly soluble on a digital computer and should be useful, along with the interval state technique suggested, in the study of the dynamic, and transients in case of symmetrical or asymmetrical operation of any inverter type and cycloconverter.

This model enables one to consider the D C linkfilter easily without approximation. The model is applied for symmetrical and asymmetrical cases. It shows that the motor torque shape is very sensitive to the asymmetry of triggering. The asymmetry of one interval led to modulation of the six pulses wave by the fundamental pulsation. The asymmetry for each interval led to a distortion of the six pulse wave. These pulsating torques may lead to higher shaft stresses and speed oscillation.

Appendix (A)

Transformation of Rotor Variables

The following equations describe the electrical operation of the induction machine in terms of the phase variables:

$$\begin{bmatrix} V_{ABC} \\ V^{r}_{abc} \end{bmatrix} = \begin{bmatrix} [R] + \mathrm{P}[\psi] \end{bmatrix} \begin{bmatrix} i_{ABC} \\ i_{abc} \end{bmatrix} \qquad (A-1)$$

Assuming a short circuited rotor, there is no zero sequence rotor voltage and hence, no zero sequence rotor current. Hence, the rotor variables are reduced to two instead of three by using the fact that

$$i^{r}_{c} = - i^{r}_{a} - i^{r}_{b} \qquad (A-2)$$

Equation (A−1) could be transformed and reduced to five variables from six, obtaining the connection matrix [C] from

$$\begin{bmatrix} i_A \\ i_B \\ i_C \\ i_{ar} \\ i_{br} \\ i_c \end{bmatrix} = \begin{bmatrix} 1 & 0 & 0 & 0 & 0 \\ 0 & 1 & 0 & 0 & 0 \\ 0 & 0 & 1 & 0 & 0 \\ 0 & 0 & 0 & 1 & 0 \\ 0 & 0 & 0 & 0 & 1 \\ 0 & 0 & 0 & -1 & -1 \end{bmatrix} \begin{bmatrix} i_A \\ i_B \\ i_C \\ i_{ar} \\ i_b \end{bmatrix} \quad (A-3)$$

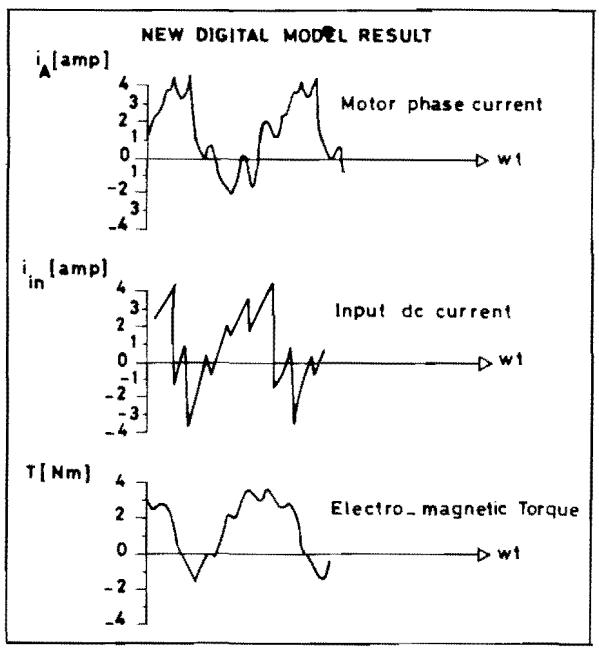

Fig. (9). Asymmetry of 12° in one interval
θ° = 1472.5 rpm f = 50 Hz E = 180 V

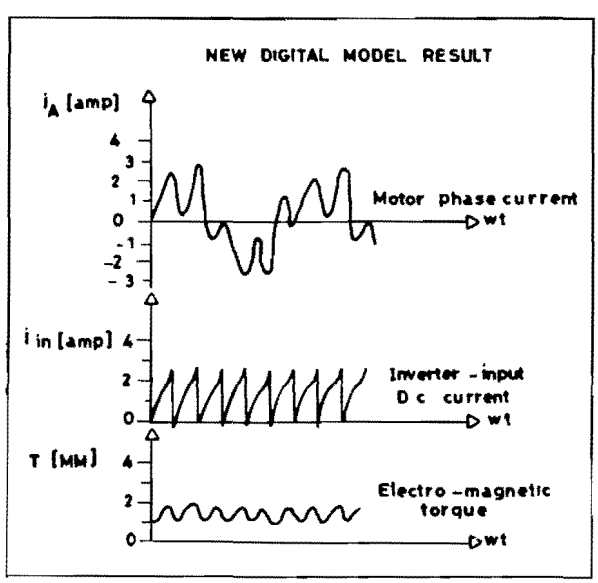

Fig. (10). Asymmetry of 2.5 in one interval
θ° = 1472.5 rpm f = 50 Hz E = 180 V

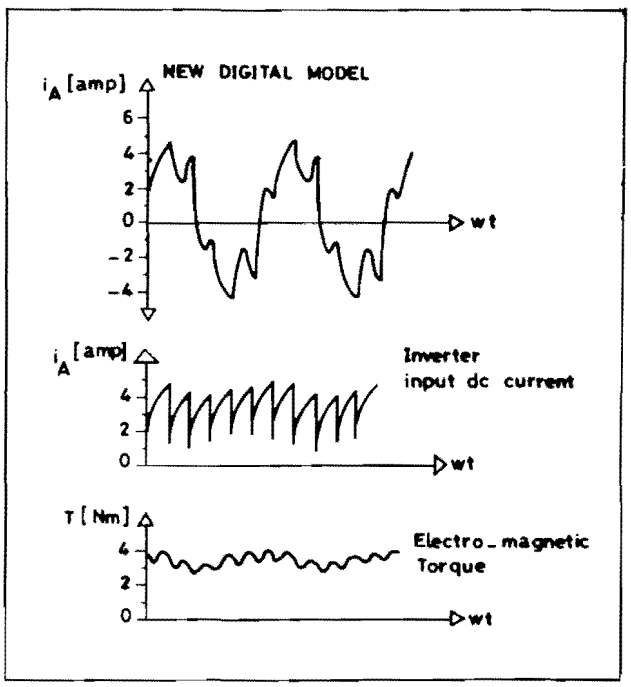

Fig. (11). Asymmetry of 2.5 in one interval
θ° = 1430 rpm f = 60 Hz E = 180 V

Then the rotor variables are changed to stationary variables. These are the current variables which, when flowing through stationary windings, produce the same rotor MMF as do the actual rotor currents. The fictitious stationary rotor coil currents are i_a, i_b, i_c,

The relation between the five variables of the current vector in equation (A-3) and the stationary A, B, C, a, b current variables is:

$$\begin{bmatrix} i_A \\ i_B \\ i_C \\ i_{ar} \\ i_{br} \end{bmatrix} = \begin{bmatrix} 0 & 0 & 0 & 0 & 0 \\ 0 & 0 & 0 & 0 & 0 \\ 0 & 0 & 0 & 0 & 0 \\ 0 & 0 & 0 & \sqrt{\frac{2}{3}}\cos(P\theta - 30) & \sqrt{\frac{2}{3}}\sin(P\theta) \\ 0 & 0 & 0 & \sqrt{\frac{2}{3}}\sin(P\theta) & \sqrt{\frac{2}{3}}\cos(P\theta + 30) \end{bmatrix} \begin{bmatrix} i_A \\ i_B \\ i_C \\ i_a \\ i_b \end{bmatrix} \quad (A-4)$$

The connection matrix for this transformation can be obtained from equation (A-4).

The stator variables can be reduced to two variables instead of three without missing the stator terminal individuality. This is done by excluding the zero sequence current of i_A, i_B, i_C to be i_α, i_β, i_γ.

By applying equation (A-2), equation (A-4) will be:

$$\begin{bmatrix} i_\alpha \\ i_\beta \\ i_\gamma \\ i^r_a \\ i^r_b \end{bmatrix} = \begin{bmatrix} 1 & 0 & 0 & 0 \\ 0 & 1 & 0 & 0 \\ -1 & -1 & 0 & 0 \\ 0 & 0 & \frac{2}{\sqrt{3}}\sin(P\theta-30) & \frac{2}{\sqrt{3}}\sin(P\theta) \\ 0 & 0 & \frac{2}{\sqrt{3}}\cos(P\theta) & \frac{2}{\sqrt{3}}\cos(P\theta+30) \end{bmatrix} \begin{bmatrix} i_\alpha \\ i_\beta \\ i_a \\ i_b \end{bmatrix} \quad (A-5)$$

When the transformations represented in equations (A−3) and (A−5), are successively applied to equation (A−1) and the zero-sequence is considered, the following equation is obtained:

$$\begin{bmatrix} V_A+V_B+V_C \\ V_A-V_C \\ V_C-V_B \\ 0 \\ 0 \end{bmatrix} =$$

$$\begin{bmatrix} 3R^s & 0 & 0 & 0 & 0 \\ 0 & 2R^s & R^s & 0 & 0 \\ 0 & R^s & 2R^s & 0 & 0 \\ 0 & 0 & \sqrt{3}Mw^r & 2R^r & R^r + \frac{3\sqrt{3}}{2} L^r_p w^r \\ 0 & -\sqrt{3}Mw^r & 0 & R^2 - \frac{3\sqrt{3}}{2} L^r_p w^r & 2R^r \end{bmatrix} \times$$

$$\begin{bmatrix} i_o \\ i_\alpha \\ i_\beta \\ i_a \\ i_b \end{bmatrix} + \begin{bmatrix} 3L_0 & 0 & 0 & 0 & 0 \\ 0 & 3L^s_p & \frac{3}{2}L^s_p & 2M & M \\ 0 & \frac{3}{2}L^s_p & 3L^s_p & M & 2M \\ 0 & 2M & M & 3L^r_p & \frac{3}{2}L^r_p \\ 0 & M & 2M & \frac{3}{2}L^r_p & 3L^r_p \end{bmatrix} P \begin{bmatrix} i_o \\ i_\alpha \\ i_\beta \\ i_a \\ i_b \end{bmatrix} \quad (A-6)$$

or

$$[V]_p = [G_{(w)r}]_p [i]_p + [L]_p P [i]_p \quad (A-7)$$

Appendix (B)

Particulars of The Induction Motor Used in Computation

Connection	Star
Rated Power, kw.	4.
Rated Voltage, Volt.	380.
Frequency, H_z.	50.
No. of poles	4
Full load stator current, Amp.	9.
Equivalent circuit parameters referred to stator, Ohm:	
R^S	1.360
R^r	1.426
$X^s_{L_r}$	2.530
$X^r_{L_r}$	2.530
X^m	69.230

8. References

1. **Charlton, W.,** Matrix method for the steady state analysis of inverter fed induction motors, *Proc. IEE,* **120,** (3), 363–365 (1973).

2. **Charlton, W.,** Matrix approach to steady state analysis of inverter fed induction motors, *Elect. lett.,* **6,** (14), 415–416 (1970).

3. **Krause, P.C.,** and Hoke, J.R., Method of multiple reference frames applied to the analysis of a rectifier inverter induction motor drive, *IEEE Trans. Power App. & Systems,* **PAS-88,** (11), 1635–1641 (1969).

4. **Lipo, T.A.,** Krause **P.C.** and Jordan, H.E., Harmonic torque and speed pulsations in a rectifier inverter induction motor drive, *IEEE Trans. Power App. & Systems,* **PAS 88,** (5), 579–587 (1969).

5. **Krause, P.C.** and Lipo, T.A., Analysis and simplified representations of a rectifier–inverter induction motor drive, *IEEE Trans. Power App. & Syst.,* **88,** (5), 588–596 (1969).

6. **Krause, P.C.,** Method of multiple reference frames applied to the analysis of symmetrical induction machinery, *IEEE Trans. Power App. & Systems.,* **PAS-87,** (1), 218–227 (1969).

7. **Klingshir E.A.** and Jordan, H.E., Polyphase induction motor performance and losses on noninusoidal voltage sources, *IEEE Trans. Power App. & Systems.,* **PAS-87,** 624–631 (1969).

8. **Jain, G.C.,** The effect of voltage waveshape on the performance of a three phase induction motor, *IEEE Trans. Power App. & Systems,* **PAS-85,** 1–6 (1969).

9. **Jocovides, L.J.** Analysis of induction motor drives with a non–sinusoidal supply voltage using Fourier analysis, *IEEE Trans. Industrial Applications,* **1A-9,** (6), 741–474 (1973).

10. **Liou, M.L.,** A Novel method of evaluating transient response, *Proc. IEEE,* **54,** (1), 20–23 (1968).

11. **Robertson, S. D. T.** and Hebbar, K., A digital model for three phase induction machines, *IEEE Trans. Power App. & Systems,* **38,** (11), 1624–1634 (1969).

12. **Jacovides, L.J.,** Analysis of a cycloconverter induction motor drive system allowing for stator current discontinuities, *IEEE Trans. Industry Applications,* **1A-9,** (2), 206–214 (1973).

تحليل نظام المحرك الحثي متغيّر الذبذبة

المرحوم محمد عباس شيمي منصور*، محمد عبد الرحمن الحيدر**، أ. فتوح***

* أستاذ سابق بقسم الهندسة الكهربائية بكلية الهندسة بجامعة الرياض.

** أستاذ مساعد بقسم الهندسة الكهربائية بكلية الهندسة بجامعة الرياض.

*** قسم الهندسة الكهربائية بكلية الهندسة بجامعة القاهرة، جمهورية مصر العربية.

تناولت أبحاث كثيرة تطوير ودراسة المولد الذبذبي لاستخدامه مع المحرك الاستنتاجي ولقد تبين من هذه الابحاث ان أداء المحرك يصحبه عزوم متذبذبة وتيارات متغيرة عن الأداء الطبيعي ولقد وضعت هذه الابحاث طرقا لدراسة هذا النظام وتبين انها ذات صعوبة في تناولها وفي دقتها خاصة بالنسبة للباحثين في هذا المجال.

في هذا البحث، اقترحت طريقة جديدة لدراسة أداء المحرك مع المتذبذب وذلك باستخدام الحاسب الالكتروني الرقمي، لذلك كان ممكنا الأخذ بالامثلة لكافة المعوقات الموجودة سواء في دائرة التيار المستمر أو التيار المتردد.

تمت دراسة المحرك معمليا وباستخدام الحاسب الرقمي ومقارنة ذلك خاصة العزوم المتذبذبة التي درسها الباحثون من الوجهة النظرية فقط.

كذلك تمت دراسة تلك النظم في المجالات غير المتوازية وذلك باستخدام الطريقة المذكورة في تلك الورقة وباستخدام الحاسب الرقمي تمت مقارنتها بالنتائج العملية.